HV 2026-15

HAF- OG VATNARANNSÓKNIR
MARINE AND FRESHWATER RESEARCH IN ICELAND

Ecological investigations on krill in Steingrímsfjörður North Iceland:
Life history and stock size in 2021-2023

Vistfræðirannsóknir á ljósátu í Steingrímsfirði:
Lífssaga og stofnstærð árin 2021-2023

Ástþór Gíslason, Páll Reynisson, Jón Örn Pálsson

HAFRANNSÓKNASTOFNUN
Rannsókna- og ráðgjafarstofnun hafs og vatna
MARINE & FRESHWATER RESEARCH INSTITUTE

Ecological investigations on krill in Steingrímsfjörður North Iceland: Life history and stock size in 2021-2023

Vistfræðirannsóknir á ljósátu í Steingrímsfirði: Lífssaga og stofnstærð árin 2021-2023.

Höfundar	Ástþór Gíslason, Páll Reynisson, Jón Örn Pálsson
Samstarfsaðilar	Ocean EcoFarm ehf
Verkefnisstjóri	Jón Örn Pálsson
Yfirfarið af	Guðmundur J. Óskarsson
Samþykkt af	Guðmundur J. Óskarsson

Haf- og vatnarannsóknir / Marine and Freshwater Research in Iceland

Númer	HV 2026-15	**ISSN**	2298-9137
Dagsetning	Mars 2026	**Dreifing**	Opin
Fjöldi síðna	21	**Verknúmer**	14916

Ágrip

Gerð er grein fyrir niðurstöðum rannsókna sem fram fóru frá maí 2021 til júní 2023 með það að markmiði að afla upplýsinga um vistfræði og magn ljósátu í Steingrímsfirði. Magn og dreifing ljósátu var metin með bergmálsaðferð (38, 120, 200 kHz) og samanburði við upplýsingar frá háfum og svifsjá. Sjávarhiti við yfirborð var ~7°C í október, ~2°C í febrúar og ~6°C í júní. Flúrljómun (mælikvarði á magn blaðgrænu) var mjög lág í október og febrúar en mun hærri í júní sem er vísbending um mikinn vöxt svifþörunga á þeim tíma. Agga (*Thysanoessa raschii*) reyndist algengasta ljósátutegundin (~48% af heildarafla allra leiðangra) en talsvert fannst líka af augnsíli (*T. inermis*, ~18%). Náttlampi (*Meganyctiphanes norvegica*) var fremur sjaldgæfur (~2%). Ljósátulirfur (furcilíu-stig) voru algengar í júní (~59-99%) sem endurspeglar að hrygning ljósátu hafi gerst nokkru fyrr, sennilega aðallega í maí. Bergmálsmælingarnar sýndu að lífmassi ljósátu var mestur í dýpstu álunum í Steingrímsfirði (dýpi > ~70-80 m). Gott samræmi reyndist á milli bergmálsmælinganna og svifsjármælinganna. Endurvarpsstuðlar ljósátu voru reiknaðir út samkvæmt tveimur aðferðum. Annars vegar var notast við svokallað DWBA-líkan (Distorted-Wave Borne Approximation) en hins vegar var gerður samanburður á milli endurvarpsgilda og mælinga á þéttleika ljósátu samkvæmt svifsjármælingunum. Samkvæmt fyrri aðferðinni var árlegur meðallífmassi ljósátu í Steingrímsfirði metinn ~8-11 þúsund tonn (meðaltal þriggja leiðangra ~10 þúsund tonn) en samkvæmt þeirri síðari ~ 6-11 þúsund tonn (meðaltal ~9 þúsund tonn). Meðalþéttleiki ljósátu samkvæmt fyrri aðferðinni var ~161 g m^{-2}, en samkvæmt hinni síðari ~144 g m^{-2}. Dægurfar ljósátu var rannsakað í júní 2023. Niðurstöður sýndu að það voru einkum stærri einstaklingarnir sem ástunduðu lóðréttar dægurgöngur upp í yfirborðslögin að nóttu til á meðan ungviðið (afkomendur vorhrygningar) hélt sig í yfirborðslögum allan sólarhringinn. Ljósáta er mikilvægur þáttur í fæðu flestra nytjastofna á svæðinu. Ef til nýtingar ljósátu kemur er því mikilvægt að fylgjast vel með hvernig ljósátustofnarnir bregðast við nýtingu.

Lykilorð: Ljósáta, bergmálsmælingar, endurvarpsstuðull, svifsjá, dægurfar

Abstract

Results are presented of a study that was carried out from May 2021 to June 2023 in Steingrímsfjörður northwest Iceland to estimate the abundance and distribution of euphausiids. It was done by acoustic surveys using echo sounders at 38, 120 and 200 kHz. Concurrent data on abundance and distribution of euphausiids were obtained by Bongo-nets and Video Plankton Recorder (VPR). Near surface temperatures were ~7°C in October, decreased to ~2°C in February and increased to ~6°C in June. Fluorometer values (an index of phytoplankton biomass) were generally very low in October and February, while much higher values were recorded in June reflecting significant phytoplankton growth. Thysanoessa raschii *was the most abundant euphausiid species (~48% of total catch of euphausiids for all the cruises combined), followed by* T. inermis *(~18%) and* Meganyctiphanes norvegica *(~2%). Euphausiids larvae (furcilia stage) were very abundant in June (~59-99%) reflecting that spawning hand taken place prior to the sampling, probably mainly in May. The acoustic measurements indicated greatest biomass of euphausiids in the middle trough of the fjord where depth was greater than ~70-80 m. Acoustic and VPR estimates of euphausiid density agreed fairly well. Biomass of krill for the whole study area based on target strength (TS) estimated by the Distorted-Wave Borne Approximation (DWBA) model ranged between ~8 and ~11 thousand tonnes wet weight with a mean value for three cruises of ~10 thousand tonnes. Values based on TS derived from matching the acoustic signals to the*

abundance of animals according to the VPR ranged between ~6 and ~11 thousand tonnes wet weight with a mean of ~9 thousand tonnes. These two approaches resulted in mean krill density of ~161 gm^{-2} and ~144 gm^{-2}, respectively. Diel variability in vertical distribution was studied in June 2023. Results show that the larger individuals of krill were those that mainly took part in vertical dial migrations to the surface layers at night, whereas the smaller ones (the juveniles from the spring spawning) tend to be concentrated in surface waters during both day and night. Euphausiids form an important component of the food of almost all utilized stocks in the region. Utilisation or harvesting of euphausiids in the fjord should therefore be paralleled by by-catch analysis and analysis of how the stocks react to the harvesting.

***Keywords**:* Euphausiids, acoustic measurements, target strength, Video Plankton Recorder, vertical diel migrations.

Table of Contents

List of figures

List of tables

1 Introduction

Krill form a large part of the marine zooplankton. They feed on phytoplankton and sometimes zooplankton and are themselves important food source for numerous species of fish, seabirds, and marine mammals. The biomass of krill within the 0.76 million square kilometres Icelandic Economic Zone (IEZ) has been estimated as 5 million tonnes wet weight constituting ~9% of the estimated combined biomass of the major components in the marine ecosystem within the IEZ (Astthorsson et al. 2007). While this can only be considered a crude estimate it nevertheless reflects the importance of krill in the Icelandic marine ecosystem.

The Ocean EcoFarm project (OEF) aims at attracting krill to cod cages by using a light source fitted to the cages. The cages were put out in Steingrímsfjörður, a fjord located on the eastern side of the Westfjord Peninsula (Figure 1). It is about 22 km long and 3 km wide at the mouth. Most of the middle trench is 130-170 m deep. Unlike several fjords in western Norway, the fjord has no threshold near the mouth.

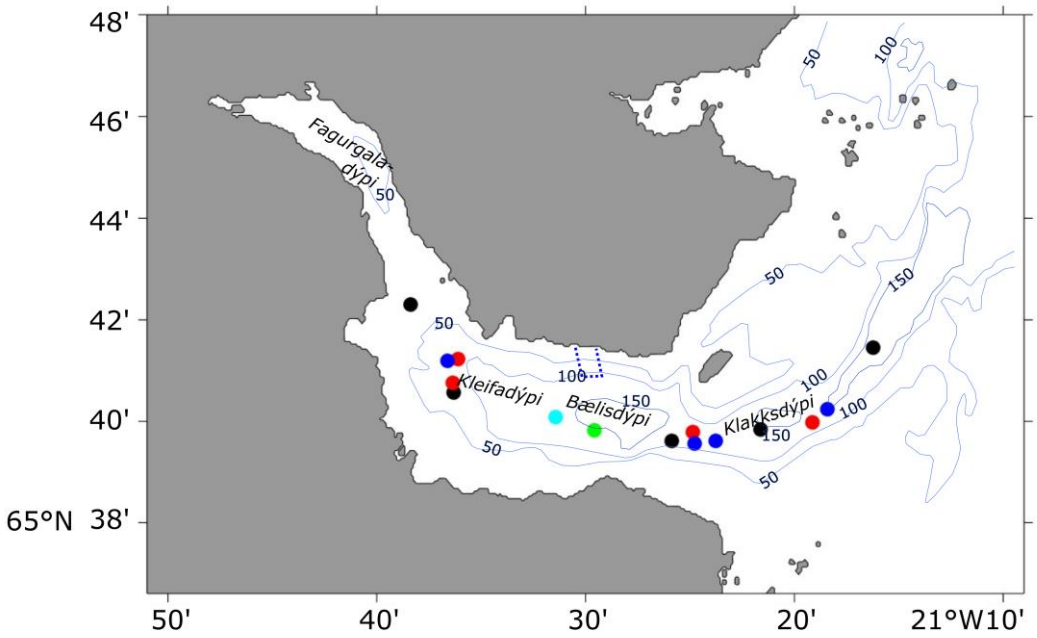

Figure 1. Map of Steingrímsfjörður showing the location of stations and the main topographic features referred to in the text. Location of the experimental area where three cages were placed is shown by the box drawn with blue broken lines. Stations are color-coded by the cruises when they were occupied: cyan (grim-02-2021), green (grim-03-2021), blue (grim-01-2022), red (grim-01-2023), black (grim-02-2023).

Experiments have shown that the submerged illumination is efficient in attracting zooplankters, especially krill (Palsson et al. 2004). Krill are an important food item for cod, especially at the younger age (Solmundsson et al. 2024). Preliminary findings indicate that the quantity of krill in the stomachs of the cod in the cages is increased significantly by using the illumination, which in turn is reflected in

the much higher growth rates of cod kept in cages with submerged illumination compared to those kept in cages that are not illuminated.

Harvesting krill by attracting them to cages has the potential of decreasing the krill stocks in the region where the cages are situated, thus decreasing the availability of krill as food for the natural inhabitants of the fjord. It is therefore important to monitor the krill stocks in the fjord while they are being utilized as food for cod in the cages.

The aim of this study was, firstly to map the regional and seasonal abundance of krill stocks in Steingrímsfjörður to evaluate where the deep ocean ranching operations should be located and, secondly, to provide background information on abundance and productivity of krill in the fjord that can form a basis for estimation on the impacts that future cod harvesting can have.

2 Methods

During 2021 to 2023, five cruises were conducted on a 21 m long local fishing boat, Grímsey ST2, in Steingrímsfjörður to investigate abundance, species composition and productivity of krill in the fjord (Figure 1, Table 1). During these cruises different gear and methodologies were employed (Table 1).

Table 1. Overview of cruises by Grimsey ST2 in Steingrímsfjörður in 2021-2023 and gear used for sampling.

Cruise id	Time	Gear
grim-02-2021	5-6 May 2021	VPR, Bongo
grim-03-2021	21-22 June 2021	VPR, Bongo
grim-01-2022	11-13 October 2022	VPR, Bongo, Acoustics
grim-01-2023	14-17 February 2023	VPR, Bongo, Acoustics
grim-02-2023	6-9 June 2023	VPR, Bongo, Acoustics

On the two cruises in 2021, activities included the towing of a Video Plankton Recorder (VPR) and the taking of samples with a Bongo net at locations where densities of krill were relatively high. On the cruises in 2022 and 2023, acoustic monitoring at three different frequencies along the sail track of the boat was added to the cruise program (Table 1).

2.1 Bongo net

The Bongo net tows were usually targeted to dense layers of krill according to the acoustic registrations. The net was lowered to a depth of relatively dense krill registrations and towed horizontally a distance of 0.5 nm at a speed of ~2 knots, thereafter it was raised to the surface and taken back on-board the ship (Tow type 10 in Wiebe et al., 2015). In the absence of acoustic registrations in 2021, the Bongo net was lowered to ~100 m depth and then heaved again while the ship sailed at slow speed (~1-2 knots) (tow type 7 in Wiebe et al. 2015). During each tow, the depth of the Bongo net was monitored with a Scanmar depth sensor fitted on the wire just above the Bongo frame. When towing the Bongo net in 2022 and 2023, four forward-looking strobe lights (Orcatorch D550) were fastened to the Bongo net frame, two on each circular opening (180° apart from each other). The light was produced by LEDs with main colour output between 420 and 650 nm (CREE XM-

L2 (U4)). Each light emits up to 1000 lumens at a blinking rate of 6 Hz. Recent studies have shown that by using strobe lights, the catch of krill is increased by reducing the avoidance behaviour of the animals rather than by attracting them (Wiebe et al. 2004, 2013, Gislason et al. 2022).

The catch was preserved in 4% neutralized formalin. Later, in the laboratory ashore, the formalin samples were analysed for species composition of krill. The length of the euphausiids was measured from a randomly selected subsample from each tow. Usually, the carapace length of the animals was measured (CL1, measured from the base of the eye-stalk to the lateral edge of the carapace, Matthews 1973, Mauchline 1980), but sometimes the total length was also measured (AT, from the anterior edge of the eye to the posterior tip of telson, excluding the setae, Mauchline and Fisher 1969). Regression analyses were used to convert carapace length (CL1) to total length (AT).

2.2 Video Plankton Recorder

A Digital Autonomous Video Plankton Recorder (DAVPR) from Seascan Inc., equipped with a camera that takes colour images at a rate of up to 15 images per second, was used to estimate the abundance and distribution of plankton and particles (Davis et al., 2004). The VPR was fitted with a SBE-49 Seabird CTD and Wetlabs ECO Puck fluorometer/turbidity sensor, by which temperature, salinity, pressure (depth), fluorescence and turbidity were measured from essentially the same parcel of water where the images were taken.

The DAVPR has four user selectable settings for field of view. For the present study, the field of view of the camera was set at 42 * 42 mm (S3), giving a calibrated image volume of 407 mL (calibrated as in Gislason et al. 2016).

The VPR frame was equipped with four forward-looking strobe lights of the same type as used on the Bongo net frame.

The VPR was usually towed by the boat in a saw-tooth trajectory (“tow-yos”) between the surface and to near the bottom (~20 m above the bottom). Sometimes the tows were targeted to the denser acoustic registrations identified as krill and then the VPR was towed more or less horizontally through the krill layers. Towing speed was generally 2.5-3.5 knots, and the vertical speed of the VPR during lowering and hauling was ~0.5-1 m sec^{-1}.

The VPR tows produce compressed data files of images as well as ancillary CTD and fluorescence data (Hu and Davis, 2006). In-focus images of plankton/particles (Regions of Interest, ROIs) and environmental data were extracted from these files using the software AutoDeck (Seascan Inc.).

The images were then analysed automatically for abundance by the software Visual Plankton following the methods of Hu and Davis (2006). For this study, all the automatic identifications were checked manually for correctness of the classifications. Besides estimating abundance of plankton, the software Visual Plankton, also estimates the biomass of plankton. This is achieved by the software counting the number of pixels in an image and by assuming the bug is a sphere, and that the area of all the pixels combined is the projected area of this sphere, bugradius (ESR, equivalent spherical radius) and bugvolume is calculated. The bugvolume is then converted to biomass assuming the density of the animals as unity for the wet mass conversion (1 mL = 1 g wet weight, Matthews and Heimdal 1980).

The ROIs are time stamped to allow merging with the data from the CTD and the fluorometer that are written to separate data files. Upon starting the survey, the clocks of the echosounder and the VPR were synchronized to the nearest second.

2.3 Acoustics

During the cruises conducted in 2022 and 2023, three transducers, 38, 120 and 200 kHz, were flush mounted on a wing-shaped plate at the end of a sturdy pole which was fastened to the side of the boat with the transducer faces at 1 m below surface. All transducers were of the split-beam type and connected to EK60 GPT transceivers (Kongsberg Simrad). Depending on noise and bottom depth the echosounders were set to 1.3 to 2 transmissions per second. The power settings recommended by Korneliussen et al. (2008) were used. A measure of the acoustic volumes are the equivalent beam angles, alternatively beam widths, provided by the manufacturer according to tank measurements before delivery. The relevant parameters for the acoustic equipment used during the surveys are listed in Table 2. The on-axis sensitivities of the echosounders were calibrated on-site the day before or during the survey, using a 38.1 mm diameter tungsten carbide standard target (Foote and McLennan, 1984; Foote et al., 1987).

Table 2. Main parameters of the transducers and transceivers of the EK60 echosounders used in the study. ψ denotes the equivalent beam angle. A pulse length of 1 ms was used in all measurements.

Frequency (kHz)	38	120	200
Transducer type	ES38-12	ES120-7	ES200-7C
Power output (W)	500	250	120
ψ (dB)	-15.8	-20.8	-20.3

The acoustic notation that follows is according to the convention described by MacLennan et al. 2000. The cruising speed was generally 7 knots during the acoustic measurements. An acoustic signal threshold of -85 to -90 dB re 1 m^{-1} was used. At this survey speed and signal threshold, noise was clearly visible, especially at the higher frequencies. This noise was not noticeable at towing speeds (1,5 - 4 knots). From time to time during the survey, noise measurements were carried out with the echo sounders in passive mode and the average signal-to-noise ratio (SNR) was estimated at each frequency. All processing of the acoustic data was carried out in Echoview (Higginbottom et al. 2000). The stochastic variability of the echoes from one transmission to the next was evened out by calculating the average volume backscattering within each 15 transmissions in the horizontal and 15 samples in the vertical (15*15 convolution). This is equivalent to around 30 m in the horizontal and 4 m in the vertical. In the following acoustic processing, SNR ≥ 3 dB was set as requirement for each frequency. Subsequently the difference in the volume backscattering strength (SV) at 38 and 120 kHz, 5 > SV120 - SV38 < 17 dB re 1 m^{-1}, was used for distinguishing the krill backscatter from those from fish and jellies. In this process a signal threshold of -90 dB re 1 m^{-1} was used for all frequencies.

A general concern when estimating the abundance of krill by acoustic surveying lies in estimating the target strength (TS) of the krill, which is crucial to the conversion of the acoustic backscatter to biomass. At least the average target strength of the krill assemblage in the area is needed.

A comparison was made of the average number of krill in a unit volume observed by the VPR to the concurrent average acoustic volume backscattering coefficient (s_v) along the VPR towing track. This method was used on similar data from Ísafjarðardjúp (Páll Reynisson et al. 2023). When matching the acoustic and optic data, the time-lag between the observations by the echo sounder and VPR were taken into consideration. This time-lag was mainly dependent of the VPR towing depth, and the distance between the vessel and the VPR was estimated to be about three times the towing depth. It is known that krill are capable of avoiding nets and approaching vehicles (Wiebe et al. 2004, 2013, Gislason et al. 2022, Reynisson et al. 2023). This avoidance reaction is pronouncedly more effective during daylight. According to studies in Ísafjarðardjúp, both the towing speed of the VPR and using forward looking lights diminish this avoidance considerably (Reynisson et al. 2023). Hence, the strobe lights were used. Based on the towing speed the number of krill counted by the VPR was adjusted accordingly. An attempt to minimize the disturbing effect of echoes from other organism was done by limiting the data to depth regions of rather high krill density. Due to the small observation volume of the VPR (407 mL), there was at most a single euphausiid in an image and usually many images without one. To average out this presence/absence effect of the euphausiid detection, 30 s averages of the optic and acoustic values were calculated for the remaining analysis. The average back scattering cross section (σ_{bs}), and consequently its logarithmic representation (TS = 10log10(σbs)), was estimated as the ratio of the averages of s_v and the number of euphausiids detected by the VPR (ind. m^{-3}).

Substantial progress has been made in the theoretical, physics-based modelling of the target strength of zooplankton (McGehee et al., 1998; review by Stanton and Chu, 2000; Lawson et al., 2006; Conti and Demer, 2006 and references therein). It has been ascertained that the backscatter from krill in captivity is mainly dependent on size and tilt angle distribution of the animals as well as their material properties and the surroundings (Foote et al. 1990, Wiebe et al. 1990, Chu et al. 1993, and McGehee et al. 1998). We used the so called DWBA-model (Distorted-Wave Borne Approximation, Stanton et al. 1998, Stanton and Chu 2000, Conti and Demer 2006, Lawson et al. 2006). The main parameters put into this model were 0° and 30° for the mean and standard deviation of the tilt angle distribution (Kristiansen and Dalen 1986) and g = 1.04, h = 1.026 for the acoustic material properties of density (g) and sound speed (h) contrasts as measured of *Thysanoessa raschii* off Norway by Køgeler et al. (1987). The resulting equation, TS(L)=49.54•log(L)-153.77, gives the target strength of a single krill, where TS is the target strength in decibels (dB) and L is its total length (AT, Mauchline and Fisher 1969) in millimetres. As the krill larvae are expected to have a negligible effect on the total acoustic backscatter, only the adults (L ≥ 17 mm) are included in the target strength model calculations.

The total acoustic abundance due to krill backscatter from each survey was estimated by the average volume backscatter within statistical rectangles times their areal (2’ longitude * 0.5’ latitude ≈ 0.5 * 0.83 nm^2) and summed up. The total number of krill was then calculated using the target strength obtained by the two above-described methods. In the subsequent biomass calculations, the relationship obtained from studies in Ísafjarðardjúp between length and dry weight was used (Gíslason et al. 2021). To convert from dry to wet weight, a ratio of 5 was assumed (Matthews and Heimdal 1980). The relationship used was the following: wet weight(mg)=$30*10^{-5}*L(mm)^{3.8763}$. The weight of each length group was estimated according to the biological samples.

To examine seasonal patterns, data from four cruises were used. They were organized in the temporal sequence 11-13 October 2022, 14-17 February 2023, 5-6 May 2021, and 6-9 June 2023, although the

data were not sampled chronologically. Although it would obviously have been desirable to survey the area chronologically, this was not possible for logistical and practical reasons.

3 Results

3.1 Environmental conditions

In October 2022, temperature was ~7°C near the surface, increased to ~8°C at 30 m depth and decreased to ~6°C near the seabed (Figure 2). In February 2023, temperatures were much lower, ~2°C in surface waters and ~3°C below 10 m depth. In June 2023, temperatures had increased, ranging from ~6°C at the surface and decreasing uniformly to ~4°C near the seabed.

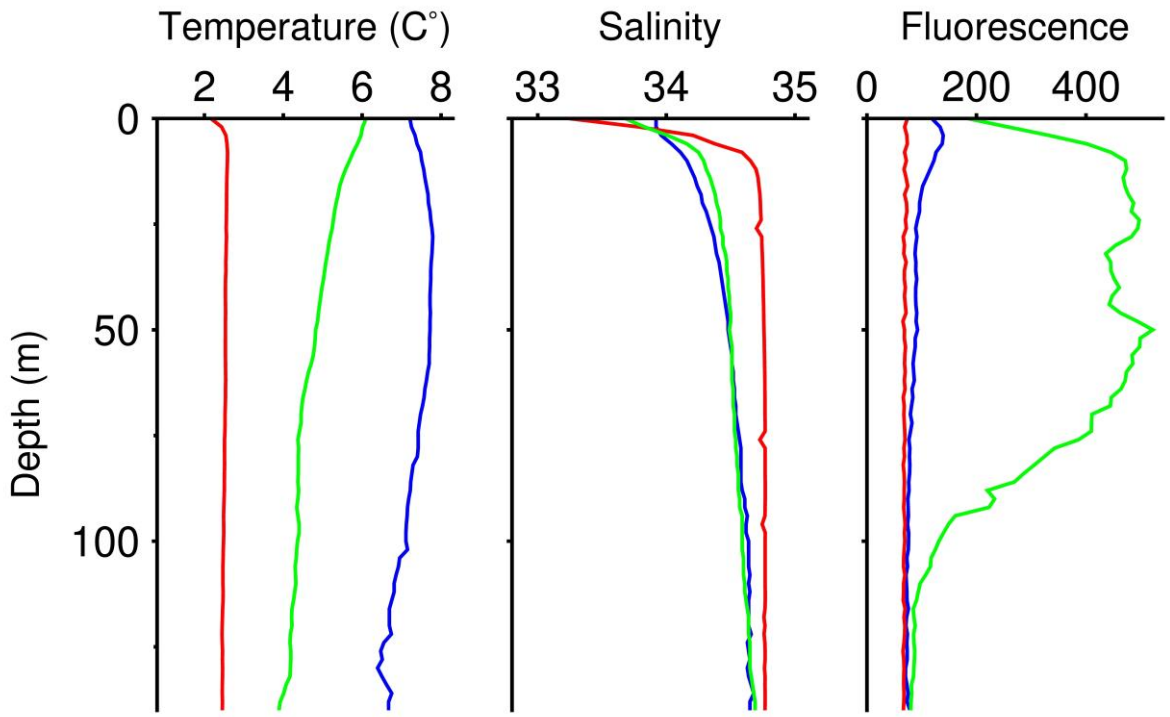

Figure 2. Vertical distribution of temperature, salinity and fluorescence (an index of Chlorophyll a concentrations) as measured by the VPR (all tows) in October 2022 (blue), February 2023 (red), and June 2023 (green).

In October 2022, salinity was lowest near the surface (~33.8) and increased evenly to the seabed (~34.7). Also in February 2023, salinity was lowest near the surface (~33.5). Salinity then increased rapidly to ~15 m depth (~34.8), below which salinity was almost constant (~34.8). In June 2023, salinity was lowest near the surface (~33) and then increased to 15 m depth (~34.4). Below 15 m depth salinity increased more slowly and was near ~34.7 near the seabed.

In October 2022, fluorometer values were generally low, while highest near the surface (5-10 m), reflecting limited phytoplankton biomass in surface waters. In February 2023, fluorescence values were even lower than in October 2022, reflecting that phytoplankton was not growing. In June 2023, the fluorescence values reflected significant phytoplankton biomass from near the surface (5-10 m depth) and to ~80-90 m depth.

3.2 Krill species

The relative species composition of krill is shown in Table 3. Adult *Thysanoessa raschii* was observed on all cruises except in June 2021. For all the cruises combined, it was the most abundant krill species (~48% by number). *T. inermis* was found in significant numbers in May 2021 (~24%), and in February 2023 when it was the most abundant species (~64%). At the other sampling times (May 2021, October 2022 and June 2023), *T. raschii* was the most abundant of identified krill species (~37-100%). *Meganyctiphanes norvegica* was observed on one cruise (February 2023, ~11%), whereas *T. longicaudata* was observed on two cruises, in June 2021 and February 2023, in low numbers (<1%).

The high proportion of unidentified furcilia larvae in June 2021 and 2023 (~59-99%) reflect that spawning had taken place prior to the sampling, probably mainly in May.

Table 3. Average species composition of krill caught by Bongo-nets in five surveys (%). The furcilia stages were not determined to species level.

Cruise id	Month	#samples	furcilia	*T. inermis*	*T. raschii*	*T. longicaudata*	*M. norvegica*
grim02-2021	May 2021	1	0	24.1	75.9	0	0
grim03-2021	Jun 2021	1	99.3	0	0	0.7	0
grim01-2022	Oct 2022	4	0	0	100	0	0
grim01-2023	Feb 2023	4	0.3	63.7	25	0.3	10.7
grim02-2023	Jun 2023	5	58.9	3.6	37.3	0.2	0
Average		15	31.7	18.3	47.6	0.2	2.1

3.3 *Thysanoessa raschii* life cycle

During most samplings in Steingrímsfjörður, the length distributions of krill were bi- or three modal indicating different year classes (Figure 3). Krill develop gonads during winter, when the females develop eggs, and the males develop sperm. The sperm is stored in special packets, called spermatophores, that are transferred to the females on copulation. The eggs become fertilized as they pass through the sperm on being released.

In the discussion below, we consider individuals to be less than one-year old (age class 0) from hatching and to end of March, one-year old from 1 April to 31 March the following year, and two-years old after that (Einarsson 1945, Falk-Petersen and Hopkins 1981, Astthorsson 1990).

In October, three length modes were observed. The smallest ones (~5-11 mm and ~13-20 mm) were juveniles from the spawning the previous spring and summer (0 group), whereas the largest length mode (~21-29 mm) were one-year old individuals.

In February, the stock consisted similarly of zero and one-year old individuals.

In May, following the notation of Einarsson (1945) mentioned above, the stock consisted of one- and two-year old individuals. High number of krill nauplii were observed during this time in the samples (data not shown) indicating that spawning was taking place.

In early June, high numbers of juveniles (furcilia ~3-8 mm long) were observed the stock. As judged by the high number of nauplii observed in May, they probably mainly hatched in May. The length modes of the one- and two-year olds had merged, probably because of mortality of part of the one-year old individuals and by their faster growth compared to the two-years old.

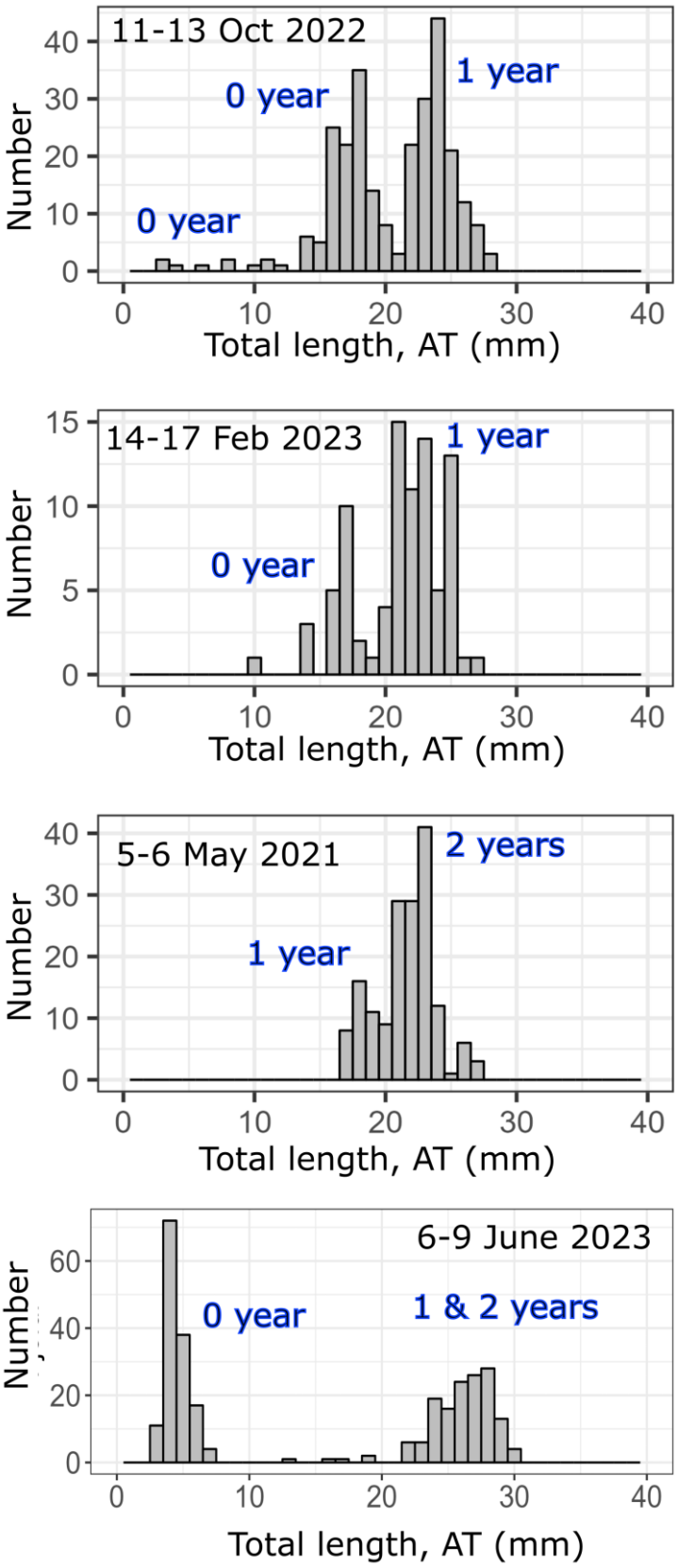

Figure 3. Length distributions of *Thysanoessa raschii* at different times of year, October 2022, February 2023, May 2021 and June 2023. Samples were collected by a 500 µ Bongo net.

Thus, the animals probably spawn first as one-year olds. Part of the stock dies afterwards, but a part grows on to become two-years old and spawn again. After the latter spawning, they die.

Simplified growth cycle of *Thysanoessa raschii* based on the length modes illustrated in Figure 3 is presented in Figure 4. The juveniles reach a length of ~15 mm during the first summer. After the first winter period they spawn in May. The krill grow then to a length of ~24 mm length as one-year olds. After the second winter period they then spawn again in May as two-year olds. Then they probably die off from the population.

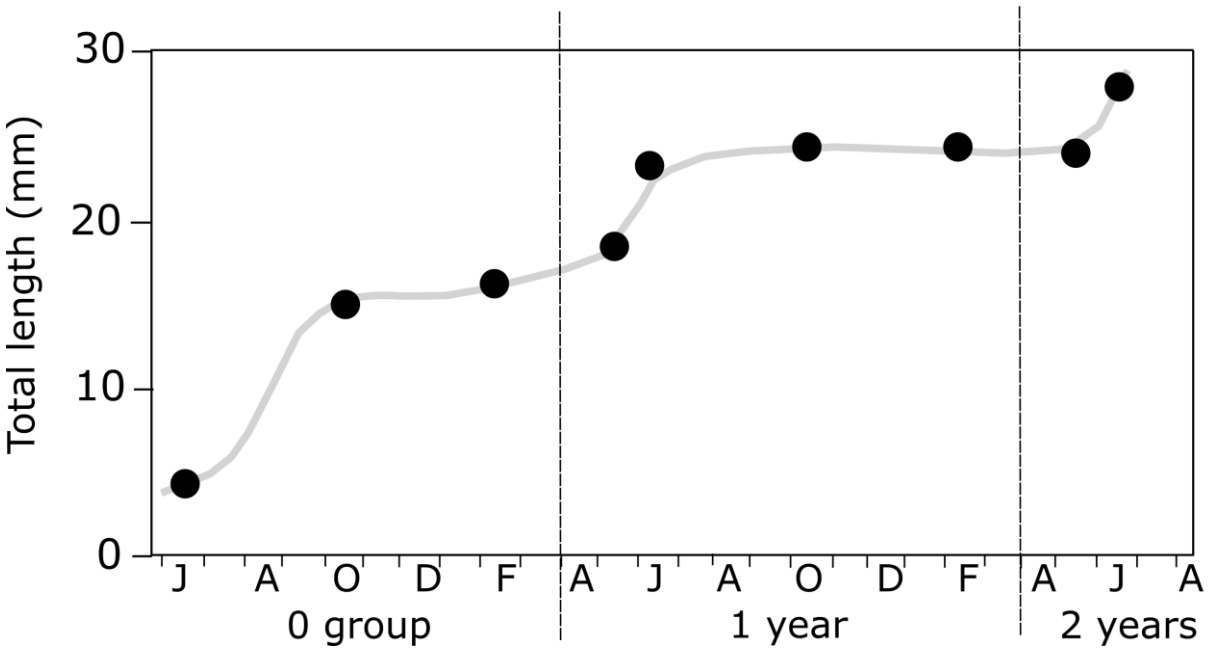

Figure 4. Simplified growth cycle of *Thysanoessa raschii* based on the length modes illustrated in Figure 3. The year classes are indicated on the figure.

3.4 Abundance and distribution of krill

In October 2022, the biomass of krill was by far the highest in Kleifadýpi (Figure 1) and diminished outwards from there. Biomass was very low over the shallow parts on both sides of the fjord (Figure 5).

In February 2023, biomass was highest in the outer parts of the fjord, in Bælisdýpi and Klakksdýpi (Figure 5). As in October 2022, very limited biomass was observed over the shallows.

In June 2023, biomass was highest in the deepest basins southeast of Grímsey, with lower values being observed in other areas, except in Kleifadýpi where significant biomass was observed. As during the other cruises where acoustics were employed, very little biomass was observed over the shallow parts of the fjord on both sides.

Figure 6 shows the relative depth distribution of krill during daytime according to the acoustic measurements. In September 2022, the bulk of the populations of krill stayed at a depth of ~60-140 m. In February 2023, the populations were found deeper (~140-170), while in June 2023, the depth distribution was somewhat similar as in September 2022 (main part at a depth of ~60-140 m).

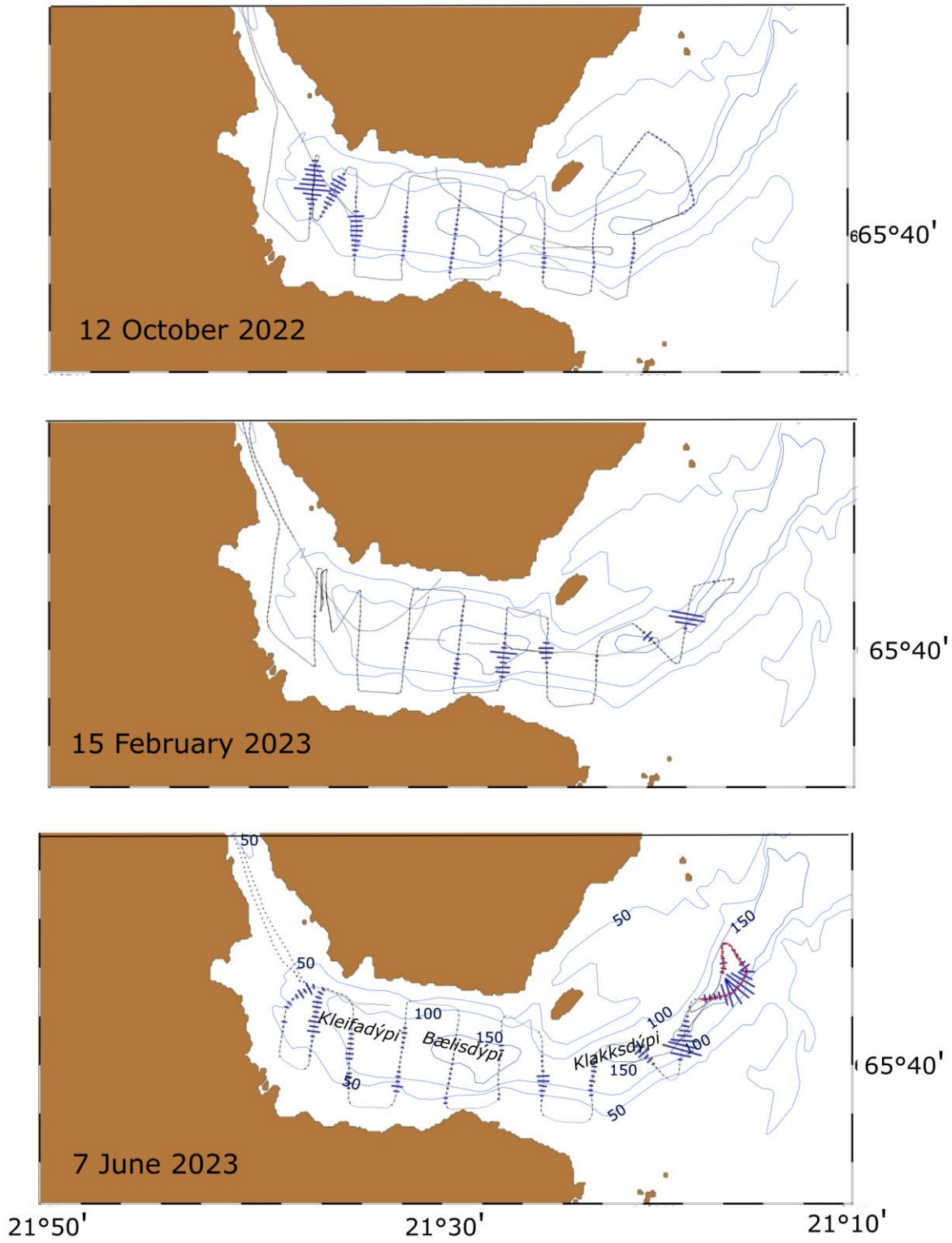

Figure 5. Distribution of krill biomass in Steingrímsfjörður 12 October 2022 (top), 15 February 2023 (middle) and 7 June 2023 (bottom) according to the acoustic measurements. Acoustic backscattering strength per 0.1 nautical mile is indicated by the length of the lines perpendicular to the cruise track. The cruise track also included sailing into the bottom of the fjord. No registrations were recorded there, and they are therefore excluded from the maps.

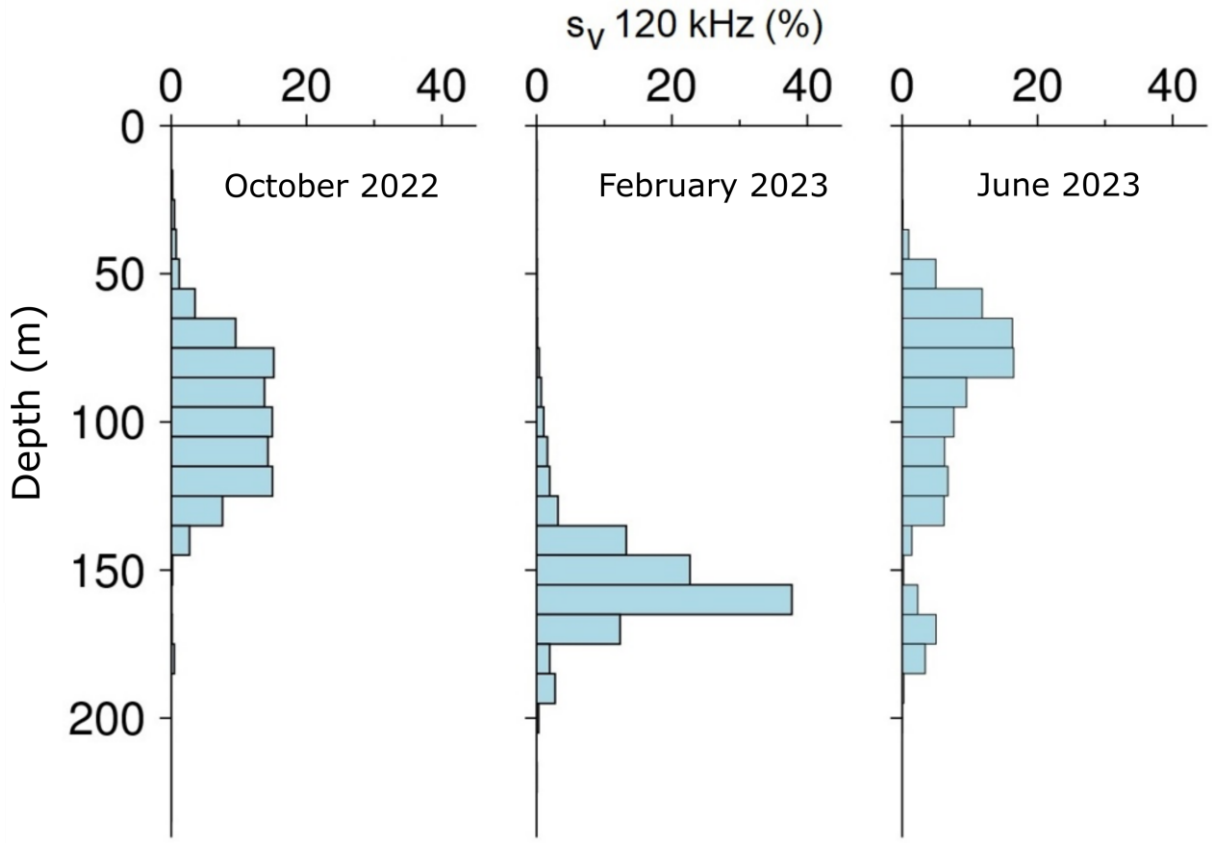

Figure 6. Vertical profiles of the acoustic values in Steingrímsfjörður at 120 khz according to measurements in October 2022, February 2023, and June 2023. The figures show average proportional values in the water column (%) within 10 m depth bins.

Estimated biomass of krill for the whole study area based on TS estimated by models ranged between ~8 and ~11 thousand tonnes wet weight with a mean value for all three cruises of ~10 thousand tonnes (Table 4). Values based on TS derived from matching the acoustic signals to the abundance of animals according to the VPR ranged between ~6 and ~11 thousand tonnes wet weight with a mean of ~9 thousand tonnes. The former biomass estimate transforms to a mean density of krill ~161 g m^{-2}, whereas the latter approach, matching the acoustics and the VPR data, gives a mean density of 144 g m^{-2} (Table 4).

3.5 Vertical distribution of main zooplankton groups

The depth distribution of krill, copepods, and jellies along a transect in the middle trough of the fjord during daytime was studied by the VPR (Figure 7). In October 2022, the krill were mainly found below 60 m depth, with highest numbers from 70 m to 140 m depth. Similarly, the copepods were also mainly found deep in the water column, with the highest numbers from ~100 m to 160 m depth. Jellies were much more evenly distributed throughout the water column. The apparent peaks in the number of krill at ~60-90 m and 120-140 m reflect relatively high numbers near the seabed.

Table 4. Krill wet weight biomass (total for all the surveyed area and per m^2) in Steingrímsfjörður on three dates. The biomass is calculated by two methods. Firstly, the biomass is calculated based on theoretical modelling for TS(L). Secondly, biomass is estimated using the mean target strength obtained from matching the acoustic backscatter to the number of krill detected by the Video Plankton Recorder (VPR), where the TS values are corrected for towing speed. See main text for how this is done.

Cruise id	Month	Area (km^{-2})	Biomass based on TS from model		Biomass based on TS from Acoustic - VPR comparison	
			Biomass (tonnes)	Density (g m^{-2})	Biomass (tonnes)	Density (g m^{-2})
grim-01-2022	Oct 2022	84.7	11032	130	11231	132.6
grim-01-2023	Feb 2023	55.2	8494	153.8	10061	182.2
grim -02-2023	Jun 2023	51.7	10406	201.2	6109	118.1
Mean			9977	161.6	9134	144.3

In February 2023, the krill were found even deeper than in October 2022, the main concentrations being observed below 150 m depth. The depth distribution of the copepods was similar with main concentrations at 140-17 m depth. Jellies were relatively rare during this time.

In June 2023, the main part of the krill population had surfaced, with highest abundance being observed from the surface and down to ~70 m depth. In contrast, the copepods were mainly found deep in the water column, with main concentrations from ~90 m to the seabed. The numbers of jellies had increased significantly from February 2023, the highest densities being found from surface and down to ~50 m depth.

Figure 8 shows the depth distribution of krill during day and night in June 2023 to illustrate dial variability in depth distribution. During day, the numerical abundance of krill was greatest above ~80 m depth, while biomass was greatest below 50 m depth. This indicates that during daytime, krill in the surface layers were mainly small animals (juveniles). During night, both numbers and biomass were concentrated to the shallow layers, above ~40 depth, indicating that the larger individuals were those that mainly took part in vertical dial migrations to the surface layers at night. The vertical distribution of size of individuals, confirms this interpretation, namely that it is mainly large krill (adults) that migrate up to the surface layers at night, while the smallest individuals (the juveniles) tend to be most concentrated in the surface layers during both day and night.

It is of interest to compare the depth distribution of the krill as obtained by the VPR and as measured by the acoustics along the VPR-track. This is shown in Figure 9. The acoustic and VPR estimates of euphausiid density agreed fairly well, especially below ~50 m depth. In June, the agreement was poor above 40 m depth when the abundance of juveniles according to the VPR in surface waters was greatest (Figures 3, 8).

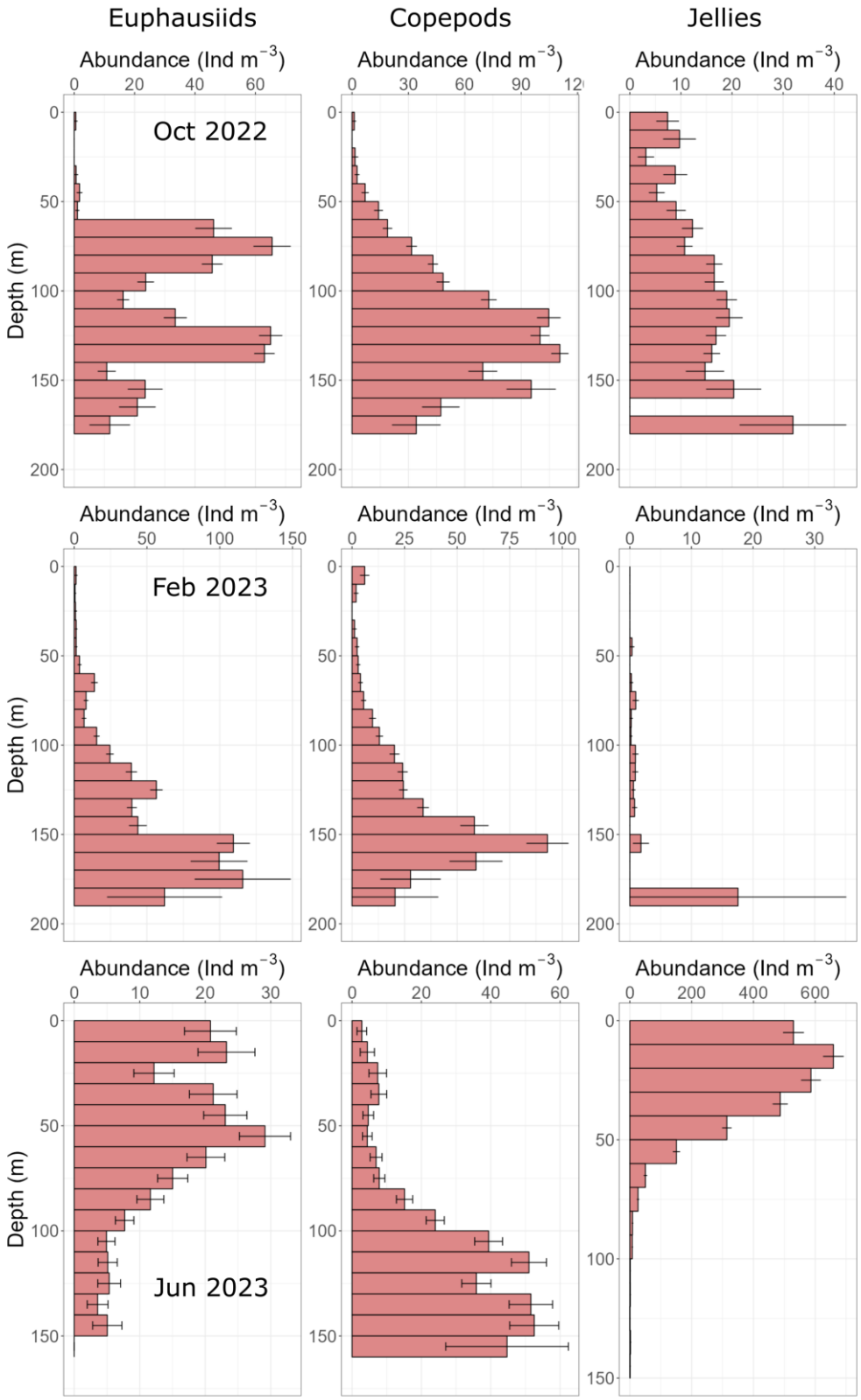

Figure 7. Vertical distribution of krill, copepods, and jellies (number m^{-3}) during daytime along a transect in the middle of Steingrímsfjörður in October 2022 (top), February 2023 (middle), and June 2023 (bottom). The figure shows average values within 10 m depth bins. The error bars are standard errors. Note that the figures are not drawn to the same scale.

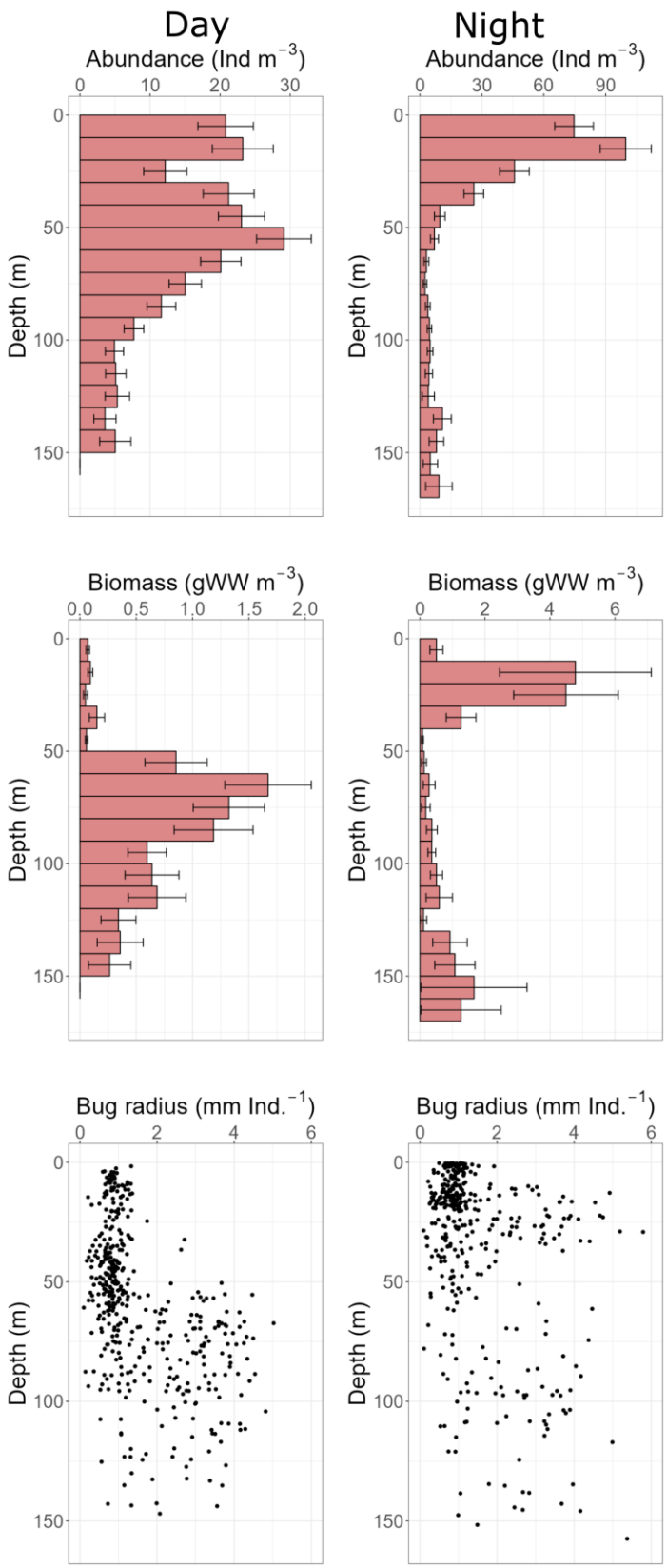

Figure 8. Vertical distribution of krill at different times of day, along a transect along the middle of Steingrímsfjörður during day and night in June 2023. The figure shows abundance (number m^{-3}, top), biomass (g wet weight m^{-3}, middle) and equivalent spherical radius (ESR) of individuals (bottom).

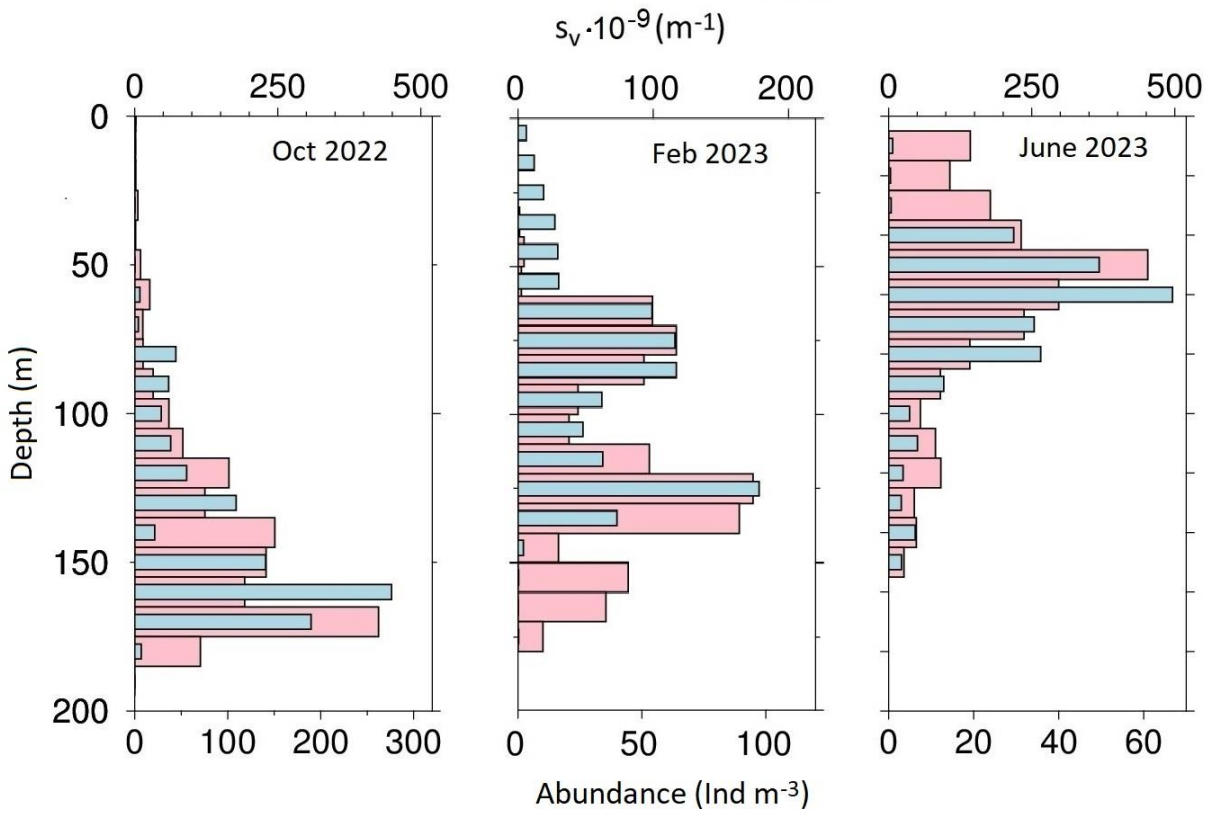

Figure 9. Vertical distribution of krill according to VPR-and acoustic analysis in Steingrímsfjörður in October 2022, February 2023, and June 2023. The figure shows average values within 10 m depth bins with number of individuals in m^3 for the VPR (red) and the volume backscattering coefficient at 120 kHz for the acoustic (blue). The VPR-values are corrected for the effect of tow-speed.

3.6 Target strength estimation of krill

The average target strength of the krill according to the comparison of the concurrent acoustic and optic observations is -87.4 dB in October 2022, -89.1 dB in February 2023 and -80.0 dB in June 2023. The 95% confidence limits of these estimates are about 0.5 dB. Accounting for uncertainties of the on-axis calibration of the echo sounder and the acoustic and optic volumes, estimated c. 6, 12 and 10% respectively, results in total uncertainty of about 1 dB, i. e. about 25% (Reynisson et al. 2023). The corresponding average TS obtained from the modelling is -87.3, -88.4 and -82.4 dB. As mentioned previously (Methods), the comparison of the acoustic-VPR data was limited by depth to the higher densities of the krill in order to minimize the disturbing effect of echoes from other organism, below 60 m depth in October 2022, below 80 m in February 2023 and 50 m in June 2023.

4 Discussion

The seasonal variability of environmental parameters and fluorescence in the fjord reported here, agrees well with an earlier annual study in the fjord made by Gudfinnsson et al. (2015). It includes the observations of the lowest temperatures in February and warming in June, and the relatively high chlorophyll values in June.

The biomass presented here on basis of acoustic measurements represents the combined biomass of all the three krill species found in Steingrímsfjörður. Biological sampling indicated that *Thysanoessa raschii* and *T. inermis* were by far the most abundant species. They are of similar size and therefore it is reasonable to assume that their TS is similar. M. norvegica was found during one cruise only. It is larger than the other two and thus probably has a larger TS. Nevertheless, in the present study we assume that all three species have the same TS.

Aside from including only krill 17 mm and larger in the model calculations, it was further assumed that the contribution from copepods to the total backscatter was negligible (could be ignored) due to their low TS (Stanton and Chu, 2000). The same is assumed for marine snow.

It has been shown that both forward looking lights and higher towing speed reduce the avoidance of the krill, and increases their apparent density as measured by the VPR. It has been estimated that a VPR towed at 3.5 knots will indicate about 70% more density as compared to towing speed of 2 knots (Páll Reynisson et al. 2023). Forward looking lights were used in all the VPR tows, but the towing speed varied from c. 1.5 to 4 knots. Within the depth ranges of interest, the average speed was around 3 knots.

The numerical agreement between target strength (TS) estimated by the Distorted-Wave Borne Approximation (DWBA) model and that derived from matching the acoustic signals to the abundance of the animals according to the VPR is satisfactory, except for the survey in June 2023. In that case the difference is markedly large, 2.4 dB or 73%. The condition of krill (e.g. fat content) varies between seasons. This could affect some parameters in the model, e. g. the g- and h-parameters and the ratio of length to girth of the krill. Adjusting these parameters could result in higher modelled-TS as compared to the parameters used and thereby a better match to the VPR-acoustic value. Another possibility is that the largest krill (modal peak at ~27 mm), avoid the VPR more effectively than the smaller adult krill (modal peak at ~20 mm). Previous studies have shown that large krill avoid nets more effectively than small krill (modal peaks ~20 and 10 mm) (Reynisson et al. 2023). Weather this applies similarly to the length groups of 20 and 27 mm krill in the case of the VPR is uncertain, but if so would result in a higher TS estimate. Nevertheless, the confidence limit for the TS obtained in June 2023 is no larger than for the other two estimates, and the same applies to the correlation between the VPR- and acoustic values depth distribution (Figure 9).

The spawning of *T. raschii* appeared to take place in parallel with the spring bloom in May. The animals spawn first as one-year olds and those that survive the spawning appear to spawn again the following spring as two-year olds. This is a similar pattern as observed in Ísafjarðardjúp (Astthorsson 1990, Gislason et al. 2021).

A factor of importance for the interpretation of the life cycle and seasonal variation in abundance and biomass is the impact that advective transport of animals may have on the life history of the krill stocks in the fjord. Krill are important part of the pelagic ecosystem around Iceland, with high abundances of animals both in the fjords and on the shelves all around Iceland (Reynisson and Gislason 2014). The question arises what relation there is between krill outside the fjord and those inside the fjord. Closest to the coast, the coastal current flows clockwise around Iceland (Valdimarsson and Malmberg 1999, Stefansson and Olafsson 1991). The mean current flows into the Húnaflói Bay on the western side and out of it on the eastern side. On entering the mouth of the Steingímsfjörður, the mean current flows

into the fjord on the northern side and out on the southern side (Macrander in preparation, Palsson et al. 2023). It is conceivable that krill would be advected by these currents both in and out of the fjord. Thus, the life cycle depicted by Figure 3 may well be confounded by the advective transports of animals. *T. raschii*, the krill species that we found in greatest overall abundance in the fjord, is regarded as a fjord species (Einarsson 1945). It is generally found in highest numbers inside fjords and in relatively low numbers outside them. Thus, this species may have evolved a behaviour that allows it to a certain degree to be retained in the fjords. It is however noteworthy that in June 2021 when furcilia larvae were very numerous, no adult *T. raschii* were found, which may mean that they were being transported by currents out of the fjord. *T. inermis* is generally regarded a shelf species (Einarsson 1945), and the fact that it disappeared twice from the samples may reflect that it is being advected in and out of the fjord by currents. *Meganyctiphanes norvegica* is usually regarded as a slope species and *T. longicaudata* as oceanic (Einarsson 1945), and their sporadic occurrence in the samples may reflect this distribution pattern.

Krill are mainly herbivorous, although they may also be carnivorous, especially during winter. M. norvegica is a more efficient carnivore than the *Thysanoessa* species, and may eat other zooplankters, like *Calanus finmarchicus* (Falk-Petersen et al. 2000, Siegel 2000, Schmidt 2010). Krill are thus generally at the base of the food web. The krill are themselves an important food source for number of marine organisms, some of which are utilized by humans, like cod, capelin, herring, saithe, whales, shrimps, and seabirds (Palsson 1983, Astthorsson and Palsson 1987, Sigurjonsson and Vikingsson 1997, Lillendahl and Solmundsson 1997, Solmundsson 2024). When evaluating the sustainability of utilizing krill as food for cod cultured in the cages.

Further, when evaluating the sustainability of krill harvesting it is important to consider not only the biomass of the krill stocks but also their production. As mentioned previously, *T. raschii* and *T. inermis* were the most abundant species in the fjord. These species have similar life cycles and are similar in size (Astthorsson 1990, Astthorsson and Gislason 1997, Silva et al. 2017). It may therefore be assumed that their productivity is similar. It is a general rule in biology that small organisms grow faster and have shorter lifespans and therefore higher turnover rates than larger organisms. The turnover rate of a population may be expressed as the relation of annual production/mean annual biomass (P/B) of the population. Banse and Mosher (1980) showed that this ratio decreases with increasing body size for several species of invertebrates, fish and mammals. This relationship ($P/B=\mu \Rightarrow P=\mu B$) has been widely used as a short-cut to estimate secondary production. For krill in northern latitudes, turnover rate values of 1.5 (Sakshaug et al. 2004) or 1.6 (Skjoldal et al. 2004) have been used. Here we use a P/B ratio of 1.5 for the combined stocks of krill. Using this ratio and the annual mean biomass estimated by our model (Table 4), the estimated annual production of krill in the fjord is ~15 thousand tonnes. This then is the result of growth and reproduction and is the amount that is available to predators without decreasing the standing stock biomass.

A prerequisite for using the P/B ratio for estimating production is that both the age structure and the size of the stock is reasonable stable. If this criterion is not met the P/B ratio will vary through the year. The criterion of a stable populations is seldom met at northern latitudes. Nevertheless, the approach of using P/B rations to estimate production is widely used in studies of northern ecosystems due to its simplicity. The current data on abundance and age structure of krill in Steingrímsfjörður show large

annual fluctuations. The production estimate given here can therefore only be considered a crude estimate of the production of krill in the fjord.

As mentioned previously, the main predators of krill in the fjord are fish, seabirds, and whales. While information on the annual consumption of these stocks in Steingrímsfjörður is not available, data from the groundfish surveys of the Marine and Freshwater Research Institute indicate that krill form a substantial part of the diet of fish in Streingrímsfjörður with around 32% of all fish caught having krill in the stomachs (Höskuldur Björnsson, verbal communication). In the much larger Ísafjarðardjúp, the annual krill consumption of cod is estimated to be 1000-2000 tonnes (Höskuldur Björnsson, verbal communication). Given the fact that Steingrímsfjörður is much smaller than Ísafjarðardjúp, it is reasonable to assume that the krill consumption by cod in Steingrímsfjörður is lower.

Whales may also be influencing the krill stocks in the Steingrímsfjörður. Humpback whales visit the Steingrímsfjörður quite frequently, and krill form an important part of their diet, particularly during summer (Gísli Vikingsson, verbal communication, Mitchell 1973 as cited in Sigurjonsson and Vikingsson 1997). Assuming that their daily consumption is ~4% of their own body weight, it may be assumed that a humpback whale weighing 20-30 tonnes would consume about 800-1200 kg per day (Þorvaldur Gunnlaugsson and Gisli Víkingsson, verbal communication). This is in general agreement with the consumption estimates given by Sigurjonsson and Vikingsson (1997).

In summary, we estimate the annual biomass of krill in Steingrímsfjörður as ~9-10 thousand tonnes wet weight. This transforms to a mean density of krill of ~144-161 g m^{-2}. In the much larger Ísafjarðardjúp, the annual biomass is much higher, ~40 thousand tonnes, whereas the density is similar (166 g m^{-2}, Gislason et al. 2021). Perhaps the mean annual density of krill is generally similar in the fjords off the northwest and north coasts of Iceland, whereas the mean annual total biomass would mainly be reflecting the different sizes of the fjords.

Acknowledgements

We want to thank Höskuldur Björnsson for digging into the data from the Icelandic groundfish surveys and Dr Gudmundur J. Oskarsson for very helpful comments on an earlier version of the manuscript.

References

Astthorsson, O. S. 1990. Ecology of the krill *Thysanoessa raschii*, *T. inermis* and *Meganyctiphane*s norvegica in Isafjord-deep, northwest Iceland. Marine Biology, 107: 147-157.

Astthorsson, O. S., Palsson, O. K. 1987. Predation on euphausiids by cod, Gadus morhua, in winter in Icelandic subarctic waters. Marine Biology, 96: 327-334.

Astthorsson O. S., Gislason, A. 1997. Biology of euphausiids in the subarctic waters north of Iceland. Marine Biology, 129: 319-330.

Astthorsson, O. S., Gislason, A., Jonsson, S. 2007. Climate variability and the Icelandic marine ecosystem. Deep-Sea Research, Part II: Topical Studies in Oceanography, 54: 2456-2477.

Banse, K., Mosher, S. 1980. Adult body mass an annual production/biomass relationships of field populations. Ecological Monographs, 50: 355-379.

Chu, D., Foote, K. G., Stanton, T. K. 1993. Further analysis of target-strength measurements of Antarctic krill at 38 and 120 kHz: comparison with the deformed-cylinder model and inference of orientation distribution. Journal of Acoustic Society of America, 93: 2985-2988.

Conti, S. G., Demer, D. A. 2006. Improved parameterization of the SDWBA for estimating krill target strength. ICES Journal of Marine Science, 63: 928-935.

Einarsson, H. 1945. Euphausiacea I. Northern Atlantic species. Dana Report, 27: 1-191.

Falk-Petersen, S., Hopkins, C. C. E. 1981. Ecological investigations on the zooplankton community of Balsfjorden, northern Norway: population dynamics of the euphausiids *Thysanoessa inermis* (Krøyer), *Thysanoessa raschii* (M. Sars) and *Meganyctiphanes norvegica* (M. Sars) in 1976 and 1977. Journal of Plankton Research, 3: 181-192.

Foote, K. G., Everson I., Watkins J. L., Bone D. G. 1990. Target strength of Antarctic krill (Euphausia superba) at 38 and 120 kHz. Journal of Acoustic Society of America, 87: 16-24.

Foote, K. G., Knudsen, H. P., Vestnes, G., MacLennan D. N., Simmonds, E. J. 1987. Calibration of acoustic instruments for fish density estimates: a practical guide. ICES Cooperative Research Report, 144: 1-69.

Foote, K. G., MacLennan, D. N. 1984. Comparison of copper and tungsten carbide calibration spheres. Journal of Acoustic Society of America, 75: 612-16.

Gislason, A. Reynisson, P. Karlsson, H., Hreinsson, E., Silva, T. Joakimsson, K., 2021. Ljósáta í Ísafjarðardjúpi – nýtanleg auðlind? (Krill in Ísafjarðardjúp, a harvestable resource? In Icelandic, English summary). Haf- og vatnarannsóknir. HV 2021-52. 43 pp.

Gislason, A., Petursdottir, H., Reynisson, P. 2023. Effect of strobe lights on catches and length distributions of euphausiids collected by Bongo nets. Journal of Plankton Research, 45: 99-109.

Gislason, Logemann, K., Marteinsdottir, G. 2016. The cross-shore distribution of plankton and particles southwest of Iceland observed with a Video Plankton Recorder. Continental Shelf Research, 123: 50-60.

Gudfinnsson, H. G., Olafsdottir, S. R., Palsson, J. Ö. 2015. Svifþörungar, næringarefni og sjávarhiti í Steingrímsfirði á Ströndum, 2010-2011. (Phytoplankton, nutrients and temperature in Steingrimsfjördur NV-Iceland 2010-2011. In Icelandic, English summary). Hafrannsóknir, 180: 1-22.

Higginbottom, I. R., Pauly, T. J., Heatly, D. C. 2000. Virtual echograms for visualization and post-processing of multiple-frequency echosounder data. In Proceedings of the Fifth European Conference on Underwater Acoustics, 10-13 July 2000, Lyon, France. Office for Publication of the European Communities, Luxembourg, pp. 1497-1502.

Hu, Q., Davis, C. 2006. Accurate automatic quantification of taxa-specific plankton abundance using dual classification with correction. Marine Ecology Progress Series, 306: 51-61.

Kristensen, Å., Dalen, J. 1986. Acoustic estimation of size distribution and abundance of zooplankton. Journal of Acoustic Society of America, 80: 601–611.

Køgeler, J. W., Falk-Petersen, S., Kristensen, Å., Pettersen, F., Dalen, J. 1987. Density and Sound Speed Contrasts in Sub-Arctic Zooplankton. Polar Biology, 7: 231-235.

Lawson, G. L., Wiebe, P. H., Ashjian, C. J., Chu, D., Stanton, T. K. 2006. Improved parameterization of Antarctic krill target strength models. Journal of Acoustic Society of America, 119: 232-242.

Lilliendahl, K., Solmundsson, J. 1997. Sumarfæða sex sjófuglategunda við Ísland. Fjölrit Hafrannsóknastofnunarinnar, 57: 249-260.

MacLennan, D. N., Fernandes, P. G., Dalen, J. 2002. A consistent approach to definitions and symbols in fisheries acoustics. ICES Journal of Marine Science, 59: 365-369.

Macrander, A. 2026. Hydrography of Steingrímsfjörður, Haf- og vatnarannsóknir, (in preparation).

Matthews, J. B. L., Heimdal, B. R. 1980. Pelagic productivity and food chains in fjord systems. In Freeland, H. J., Farmer, D. M., Levings, C. D. (Eds) Fjord Oceanography. Plenum Press, New York, 377-398.

Matthews. J. B. L. 1973. Ecological studies on the deep-water pelagic community of Korsfjorden, western Norway. Population dynamics of *Meganyctiphanes norvegica* (Crustacea, Euphausiacea) in 1968 and 1969. Sarsia, 54: 75-90.

Mauchline, J. 1980. The Biology of Mysids and Euphausiids. Blaxter JHS, Russell SFS and Yonge SM, editors. London and New York: Academic Press, 1980.

Mauchline, J., Fisher, L. R. 1969. The biology of euphausiids. Russell Frederick S. Sir and Yonge Sir Maurice, editor London and New York: Academic Press, 1969.

McGehee, D. E., O'Driscoll, R. L., Martin Traykovski, L. V. 1998. Effects of orientation on acoustic scattering from Antarctic krill at 120 kHz. Deep Sea Research Part II, 45: 1273-1294.

Palsson, J. Ö., Vidar, S., Arnarsson, Ö. G. 2024. Deep Sea Ranching. Experimental results 2021-2023. Cod growth and Pray consumptions. Work Report - Ocean EcoFarm ehf. Iceland. Confidential Document until 2027. 34 p.

Palsson, O. K. 1983. The feeding habits of demersal fish species in Icelandic waters. Rit fiskideildar, 7: 1-60.

Reynisson, P., Gislason, A. 2014. Bergmálsmælingar á ljósátu við Ísland árin 2011-2014 (Acoustic measurements of euphausiids around Iceland 2011-2014. In Icelandic, English summary). Hafrannsóknir, 81: 26-35.

Reynisson, P, Gislason, A., Lawson, G. L. 2023. Concurrent observations of the euphausiid *Thysanoessa raschii* in an Icelandic fjord by acoustics and Video Plankton Recorder: comparisons with theoretical models of target strength. Journal of Plankton Research, 45: 37-51.

Sakshaug, E., Björge, A., Gulliksen, B., Loeng, H., Mehlum, F. 1994. Structure, biomass distribution, and energetics of the pelagic ecosystem in the Barents Sea: A synopsis. Polar Biology, 14: 405-411.

Sigurjonsson, J., Vikingsson, G. 1997. Seasonal Abundance of and Estimated Food Consumption by Cetaceans in Icelandic and Adjacent Waters. Journal of Northwest Atlantic Fishery Science, 22: 271-287.

Silva, T., Gislason, A., Astthorsson, O. S., Marteinsdottir, G. 2017. Distribution, maturity and population structure of *Meganyctiphanes norvegica* and *Thysanoessa inermis* around Iceland in spring. Plos One, 12(11), 21pp.

Simmonds, E. J., MacLennan, D. N. 2005. Fisheries Acoustics: Theory and Practice. Blackwell Science, Oxford. 437 pp.

Skjoldal, H. R., Dalpadado, P., Dommasnes, Å. 2004. Food webs and trophic interactions. In Skjoldal, H. R., Sætre, R., Færnö, A., Misund, O. A., Röttingen, I. (Eds). The Norwegian Sea Ecosystem. Tapir Academic Press. Bergen.

Solmundsson, J., Björnsson, H., Jónsdóttir, I. G., Jakobsdóttir, K. B. 2024. Fæða 26 tegunda botnfiska á Íslandsmiðum árin 1996-2023. (Diet of 36 groundfish species in Icelandic waters 1996-2023. In Icelandic, English summary). Haf- og vatnarannsóknir. HV 2004-01: 156 pp.

Stanton, T. K., Chu, D. 2000. Review and recommendations for the modelling of acoustic scattering by fluid-like elongated zooplankton: euphausiids and copepods. ICES Jounal of Marine Science, 57: 793-807.

Stanton, T. K., Chu, D., Wiebe, P. H. 1998. Sound scattering by several zooplankton groups. II. Scattering models. Journal of Acoustic Society of America, 103: 236–253.

Stefansson, U., Olafsson, J. 1991. Nutrients and fertility of Icelandic waters. Rit Fiskideildar, 7: 1-56.

Valdimarsson, H., Malmberg, S, A. 1999. Near-surface circulation in Icelandic waters derived from satellite tracked drifters. Rit Fiskideildar, 16: 23–39.

Wiebe, P. H., Greene, C. H., Stanton, T. K., Burczynski, J. 1990. Sound scattering by live zooplankton and micronekton: Empirical studies with a dual-beam acoustical system. Journal of Acoustic Society of America, 88: 2346– 2360.

Wiebe, P. H., Ashjian, C., Gallager, S., Davis, C., Lawson, G., Copley, N. 2004. Using a high-powered strobe light to increase the catch of Antarctic krill. Marine Biology, 144: 493-502.

Wiebe, P. H., Lawson, G. L., Lavery, A. C., Copley, N. J., Horgan, E., Bradley, A. 2013. Improved agreement of net and acoustical methods for surveying euphausiids by mitigating avoidance using a net-based LED strobe light system. ICES Journal of Marine Science, 70: 650–664.

HAFRANNSÓKNASTOFNUN

Rannsókna- og ráðgjafarstofnun hafs og vatna